environmental microbiology

Environmental Microbiology (2020) **22**(5), 1847–1860 doi:10.1111/1462-2920.14942

Transcriptional response of *Emiliania huxleyi* under changing nutrient environments in the North Pacific Subtropical Gyre

Harriet Alexander,[1] **Mónica Rouco**,[2,3] **Sheean T. Haley**[2] **and Sonya T. Dyhrman**[2,3*]

[1]*Biology Department, Woods Hole Oceanographic Institution, Woods Hole, MA, 02543, USA.*

[2]*Biology and Paleo Environment Division, Lamont-Doherty Earth Observatory, Columbia University, Palisades, NY, 10964, USA.*

[3]*Department of Earth and Environmental Sciences, Columbia University, Palisades, NY, 10964, USA.*

Summary

The widespread coccolithophore *Emiliania huxleyi* is an abundant oceanic phytoplankton, impacting the global cycling of carbon through both photosynthesis and calcification. Here, we examined the transcriptional responses of populations of *E. huxleyi* in the North Pacific Subtropical Gyre to shifts in the nutrient environment. Using a metatranscriptomic approach, nutrient-amended microcosm studies were used to track the global metabolism of *E. huxleyi*. The addition of nitrate led to significant changes in transcript abundance for gene pathways involved in nitrogen and phosphorus metabolism, with a decrease in the abundance of genes involved in the acquisition of nitrogen (e.g. N-transporters) and an increase in the abundance of genes associated with phosphate acquisition (e.g. phosphatases). Simultaneously, after the addition of nitrate, genes associated with calcification and genes unique to the diploid life stages of *E. huxleyi* significantly increased. These results suggest that nitrogen is a major driver of the physiological ecology of *E. huxleyi* in this system and further suggest that the addition of nitrate drives shifts in the dominant life-stage of the population. Together, these results underscore the importance of phenotypic plasticity to the success of *E. huxleyi*, a characteristic that likely underpins its ability to thrive across a variety of marine environments.

Received 12 July, 2019; revised 20 December, 2019; accepted 23 December, 2019. *For correspondence.*E-mail sd2512@columbia.edu; Tel. (+845) 365 8165; Fax (+845) 365 8163

Introduction

Phytoplankton account for nearly half of global primary production (Field, 1998), exerting profound control over the global carbon cycle. The growth of phytoplankton in many parts of the well-lit surface waters of the open ocean is constrained by the supply of macronutrients, especially nitrogen (N) (Moore *et al*., 2013). It is predicted that changes in the climate and subsequent ocean warming may alter ocean circulation, directly impacting the supply of key macronutrients to surface waters and consequently phytoplankton production (Sarmiento *et al*., 1998; Behrenfeld *et al*., 2006). Such shifts in ocean circulation may lead to the expansion of N-limited subtropical gyres (Sarmiento *et al*., 2004; Polovina *et al*., 2008). Simultaneously, anthropogenic activity is shifting the sources and avenues of nutrient input into the ocean, with increasing amounts of atmospheric anthropogenic fixed nitrogen being supplied to the open ocean (Duce *et al*., 2008) and increasing amounts of riverine phosphorus inputs to coastal waters (Smil, 2000; Ruttenberg, 2001; Paytan and McLaughlin, 2007). Consequently, understanding the response of phytoplankton communities to changes in their geochemical environment is crucial for better predicting the structure and function of ecosystems in the future ocean.

Coccolithophores are a biogeochemically significant phytoplankton functional group, playing a major role in marine biogeochemical cycles, particularly in those of carbon and sulfur (Simó, 2001). Beyond their contributions to primary production (1%–10% of total marine carbon fixation), coccolithophores are a major source of particulate inorganic carbon in the form of calcite ($CaCO_3$) and are estimated to comprise about 50% of calcite deposition to sediments (Poulton *et al*., 2007). Consequently, coccolithophores play a dual role in the cycling of carbon, both in the organic carbon pump, drawing CO_2 out of the atmosphere, and the carbonate counter pump, where CO_3^{2-} removed for calcification

increases total alkalinity, leading to a positive feedback on atmospheric pCO_2 (Zondervan *et al*., 2001). The balance between calcification and carbon fixation has been found to vary across environmental factors such as temperature, salinity, light, and nutrients (Paasche, 2002; Bollmann and Herrle, 2007; Zondervan, 2007; Feng *et al*., 2008).

Emiliania huxleyi is an abundant and cosmopolitan coccolithophore capable of forming large blooms in diverse oceanic environments, ranging from coastal waters to the open ocean (Holligan *et al*., 1993; Brown and Yoder, 1994; Read *et al*., 2013). Studies on cultured isolates suggest that *E. huxleyi* strains have considerable metabolic plasticity, modulating cellular quotas (van Mooy *et al*., 2009; Shemi *et al*., 2016) and altering phenotype to scavenge nutrients from organic compounds that are typically at higher concentrations than inorganic nutrients in the upper water column (Palenik and Henson, 1997; Dyhrman and Palenik, 2003; Bruhn *et al*., 2010; Rouco *et al*., 2013; Rokitta *et al*., 2014). The metabolic plasticity of this species may be central to its cosmopolitan distribution and ability to bloom under variable conditions. Until quite recently, however, assessing the physiological response of individual taxonomic groups in mixed natural communities was intractable.

Here, we examined the metabolic plasticity of *E. huxleyi* in the North Pacific Subtropical Gyre (NPSG), building off of previous work which identified phylum-specific transcriptional patterns and their relation to ecological traits in a simulated deep water upwelling experiment (Alexander *et al*., 2015). Analysis of metatranscriptomic data from the deep water addition suggested that there were fundamental differences in the metabolic strategies of haptophytes compared to diatoms. These shifts in physiology were linked to apparent changes in the relative abundance of diatoms but not haptophytes, where *E. huxleyi* consistently recruited the most sequence reads both *in situ* and in the experimental treatment. The consistent dominance of *E. huxleyi* in both the oligotrophic surface samples and deep water amended treatments again pointed to the potential importance of its physiological plasticity in its success across environmental conditions.

In this study, we used a semi-factorial nutrient-amendment experiment to examine *E. huxleyi* metabolic plasticity in the NPSG during the summer of 2012. Compiling a reference database of the *E. huxleyi* CCMP 1516 genome (Read *et al*., 2013) and transcriptome assemblies from the Marine Microbial Eukaryotic Transcriptome Sequencing Project (MMETSP) (Keeling *et al*., 2014), the transcriptional patterns of *E. huxleyi* were identified and used as a proxy for changes in metabolism across replicated experiments designed to evaluate *E. huxleyi* responses to shifts in nutrient availability.

Results and discussion

Field sampling

Seawater for nutrient amendment microcosm experiments was collected at Station ALOHA (22°45' N, 158°00' W) from a depth of 25 m at 1400 h (local time) on 6 August (E1) and 24 August (E2) during the summer of 2012 as part of the HOE-DYLAN research expedition described by Wilson *et al*. (2015). The sampling for this study took place during a period of particularly low productivity where the mixed layer was typified by a heterotrophic state (Wilson *et al*. 2015). *Emiliania huxleyi* has been found to be consistently present, although at low abundance in sampling at Station ALOHA ranging in concentration from 1×10^3 to 20×10^3 cells L^{-1} (Cortés *et al*., 2001). During this study, the haptophyte indicator pigment 19′-hexanolyoxyfucoxanthin, which can serve as a proxy for relative haptophyte abundance, was stable across the sampling period (Wilson *et al*. 2015). Two 7-day nutrient amendment microcosm experiments were performed with 20 L of water in triplicate for the following treatments: the addition of nitrate (+N), the addition of phosphate (+P), the addition of key macro- and micronutrients except for nitrate (–N), the addition of key macro- and micronutrients except for phosphate (–P), and the addition of 10% v/v deep seawater (+DSW) as described in the study by Alexander *et al*. (2015), and a no addition control. The –N and –P treatments were designed to drive the community to draw down any available N or P, respectively, through the addition of other nutrients, while the +N and +P were designed to supply that nutrient in abundance. Although there was a consistent draw down of nutrients in the +N and +P treatments for each experiment, there was residual nitrate + nitrite (+N) and phosphate (+P) in these treatments at the time of the metatranscriptome sampling (Supporting Information Fig. S1). Chlorophyll *a* increased significantly relative to *in situ* values (T_0) and the unamended controls in all treatments where nitrate was added (+N, –P, and +DSW) (Supporting Information Fig. S2). Amended microcosm experiments were sampled on day 7 for metatranscriptomic analyses.

Physiological ecology of E. huxleyi

To capture a holistic view of the physiology of the *E. huxleyi* population in the field, all reads mapping to a custom *E. huxleyi* reference database (regardless of strain) were tracked by common orthologous group (OG). Here, a conservative approach was taken, where the two replicated experiments that were performed 2 weeks apart with different initial communities were treated as biological replicates, and significant differences in OG abundance were identified in each of the amended microcosm treatments relative to the unamended control

treatment. Gene-wise dispersion of gene counts between treatments was calculated with edgeR; thus, an OG or transcript would only be considered differentially abundant if it displays a similar pattern of abundance in the treatments being compared between the two replicated experiments. A total of 56 647 OGs were identified (Supplementary Dataset S1), and 46 064 of those were found to be expressed in one of the amended microcosm treatments (Supplementary Dataset S2). Comparisons of each of the N-amended treatments (+N, −P, and +DSW) relative to the unamended control revealed between 1212 and 1466 differentially abundant OGs [false discovery rate (FDR) <0.05], whereas non-N-amended treatments (+P and −N) had at most two differentially abundant OGs relative to the unamended control (Fig. 1 and Supplementary Dataset S3). This shift in metabolism is consistent with growth responses in the bulk community, as an increase in chlorophyll was observed in treatments amended with N (Supporting Information Fig. S2). The significantly differentially abundant OGs for the three treatments that received nitrate were conserved, with 45% of differentially abundant OGs common across the three treatments (Fig. 1F). Differential abundance analysis of the strain-specific transcripts within OGs yielded fewer differentially abundant transcripts (161–918) (Supporting Information Fig. S3 and Supplementary Dataset S4). This is likely due to a lack of statistical power, in that the read coverage of transcripts corresponding to individual strains was necessarily lower than the read coverage of OGs from the *E. huxleyi* combined database. Because of this, the following sections focus on the expression of OGs, which consider the global signature of metabolic plasticity across all the strains.

Nitrogen scavenging and assimilation

Broadly, OGs associated with N-metabolism that were significantly differentially abundant in N-amended microcosms relative to the unamended control could be broken

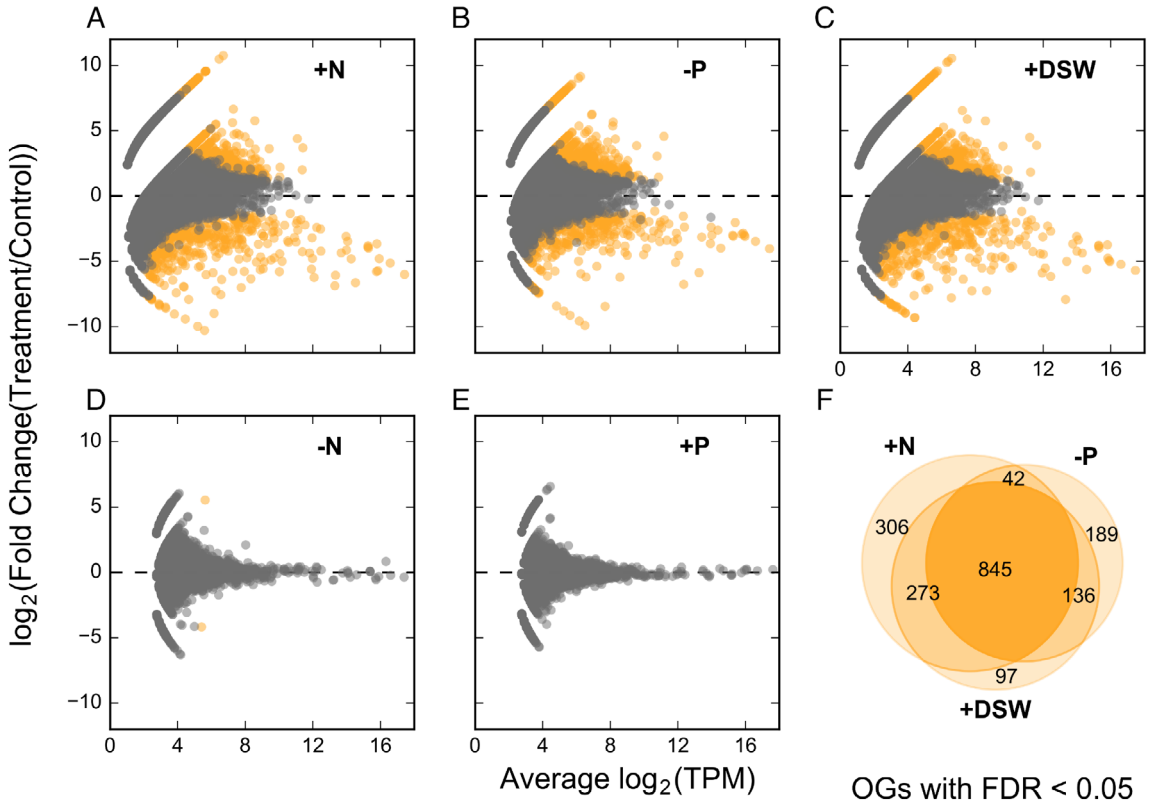

Fig. 1. The addition of nitrogen induces conserved shifts in *E. huxleyi* transcription. (A–E) Statistical significance of the log average abundance and log fold change for each of the detected *E. huxleyi* OGs was assessed between the unamended control relative to the treatments: (A) +N, (B) −P, (C) + DSW (deep seawater), (D) −N, and (E) +P. OGs that are identified as significantly increased or decreased, with a false discovery rate (FDR) < 0.05, in a treatment relative to the control are highlighted in orange while those not significantly changed are coloured grey. (F) A weighted Venn diagram comparing the composition of the significantly (FDR < 0.05) differentially abundant OGs across each of the amendments to which N was added (A–C) compared with the unamended control, with the size of the circles scaled to the relative number of differential OGs.

into two groups: OGs associated with the response to N-limitation and OGs associated with the response to newly available substrates produced over the course of the experiment, such as ammonium. In N-amended microcosms, a number of gene families that are known to be regulated by N supply had decreased abundance. For example, transporters of organic and inorganic N sources were significantly decreased (FDR <0.05) relative to the unamended control (Fig. 2). This included a family of urea transporters (UTP), ammonium transporters (AMT), and nitrate transporters (NRT) (Fig. 2 and Supplementary Dataset S3 and S5). In addition to the decreases in UTP, urease (URE), which scavenges N in the form of NH_4^+ from urea, was significantly decreased following N-addition. The largest decrease in N-metabolism-related transcripts was observed in three OGs of amidases (AMD) and formamidases (FMD), which scavenge NH_4^+ from amides and formamides (Fig. 2). These patterns were found to persist not only across the two replicated experiments but also across treatments, with many of the OGs found to be significantly regulated in more than one N-amended treatment (e.g. +DSW, −P, and +N) (Fig. 2). The decrease in FMD in the presence of nitrate has been previously observed in the laboratory (Bruhn *et al*., 2010) and an increase in a putative AMD has also been previously observed upon the termination of an *E. huxleyi* bloom (Landry *et al*., 2009), when inorganic nitrogen concentrations were low. These data suggest that *E. huxleyi*,

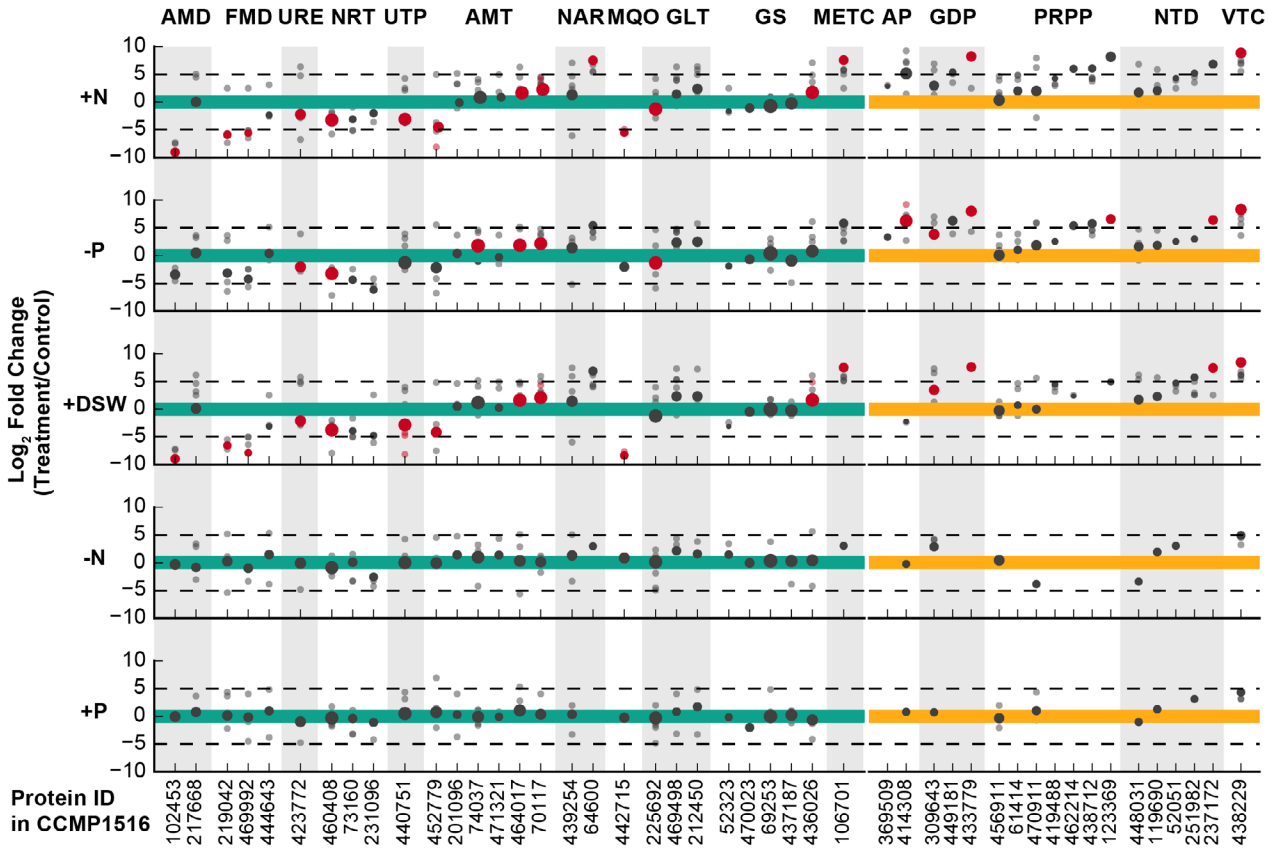

Fig. 2. Fold change of OGs associated with nitrogen and phosphorus metabolism in each of the amended microcosm treatments compared to the unamended control. The significance of log fold change of OGs associated with nitrogen (N) metabolism (teal) and phosphorus (P) metabolism (orange) (Supplementary Dataset S5) was assessed with edgeR across the five amended treatments relative to the unamended control. The size of the OG marker is proportional to the log of the mean abundance between the treatment and unamended control. OGs identified as significantly differently abundant between the treatment and the control, with a false discovery rate (FDR) < 0.05, are highlighted in red, whereas all others are plotted in dark grey. Individual transcripts within each OG are plotted in line vertically with the marker for the OG in either light grey or light red. As with the OGs, individual transcripts are highlighted in red if they are significantly differentially abundant between samples (FDR < 0.05). The x-axis labels indicate a representative protein id from the genome strain CCMP1516 for each of the OGs. OGs are grouped based on their general functions, which are listed as abbreviations across the top of the plot and alternately shaded in grey to aid visualization. These gene sets were chosen based on genes identified by McKew *et al*. (2015) and Rokitta *et al*. (2014). The abbreviations are as follows: acetamidase/amidases (AMD), formamidase (FMD), urease (URE), nitrate transporter (NRT), urea transporter (UTP), ammonium transporter (AMT), formate/nitrite transporter (NAR), malate quinone oxioreductase (MQO), glutamate synthase (GLT), glutamine synthase (GS), cystathionine beta-lyase (METC), alkaline phosphatase (AP), glycerophosphoryl diester phosphodiesterase (GDP), phosphate-repressible phosphate permease (PRPP), 5′-nucleotidase (NTD), vacuolar transport chaperone (VTC).

like many other phytoplankton (Frischkorn *et al*., 2014), might have a transcript-based nitrogen preference hierarchy, prioritizing inorganic versus organic forms of nitrogen.

There was a strong correlation between the patterns of transcript abundance observed in this study for each of the aforementioned gene families and prior transcriptomic (Rokitta *et al*., 2014) and rate-based (Palenik and Henson, 1997; Bruhn *et al*., 2010) studies focused on N-limitation responses. Most striking, however, is the coordination of each of these markers with a lab-based proteomic study of the physiological response of CCMP1516 to N limitation (Fig. 3A) (McKew *et al*., 2015). The AMT, NRT, UTP, URE, and FMD OGs observed to be less abundant in N-amended treatments were each significantly increased in the proteome of N-limited cultures of CCMP1516 (Fig. 3A). This pattern of regulation in URE was also observed at the transcript level in N-limited cultures of *E. huxleyi*, where the enzyme may serve as a means of accessing N from the ornithine-urea cycle (Rokitta *et al*., 2014) or as a means of accessing exogenous urea (Dyhrman and Anderson, 2003). *E. huxleyi* is known to grow on amides and other organic N sources (Palenik and Henson, 1997), and N-limiting conditions are known to yield increases in transcripts and enzyme activity for the AMD/FMD (Palenik and Henson, 1997; Landry *et al*., 2009; Bruhn *et al*., 2010). The data from this field study combined with many previous lab-based studies suggest that these N limitation responses are highly conserved across strains and between environmental and laboratory conditions (Figs. 3 and 4).

Differential expression patterns in the microcosms indicate further changes in N assimilation and energy production following the addition of N to the microcosms. A shift from the smaller glutamine synthase (GS) type II in treatments not amended with N to the larger GS type III with a higher N requirement was observed following N-addition (Fig. 2). Thus, the NH_4^+ released by FMD, AMD, and URE is ultimately incorporated into biological material through GS (Rokitta *et al*., 2014). In culture transcriptome comparisons, Rokitta *et al*. (2014) noted that *E. huxleyi* induces a malate:quinone-oxidoreductase (MQO) that can bypass malate-dehydrogenase (MDH) in the TCA cycle and feed electrons directly into the electron transport chain to enable the production of ATP. MQO was significantly decreased (between 5 and 9 log fold change) in both +N and +DSW (Fig. 2). The MQO, absent from diatom genomes but found to be highly

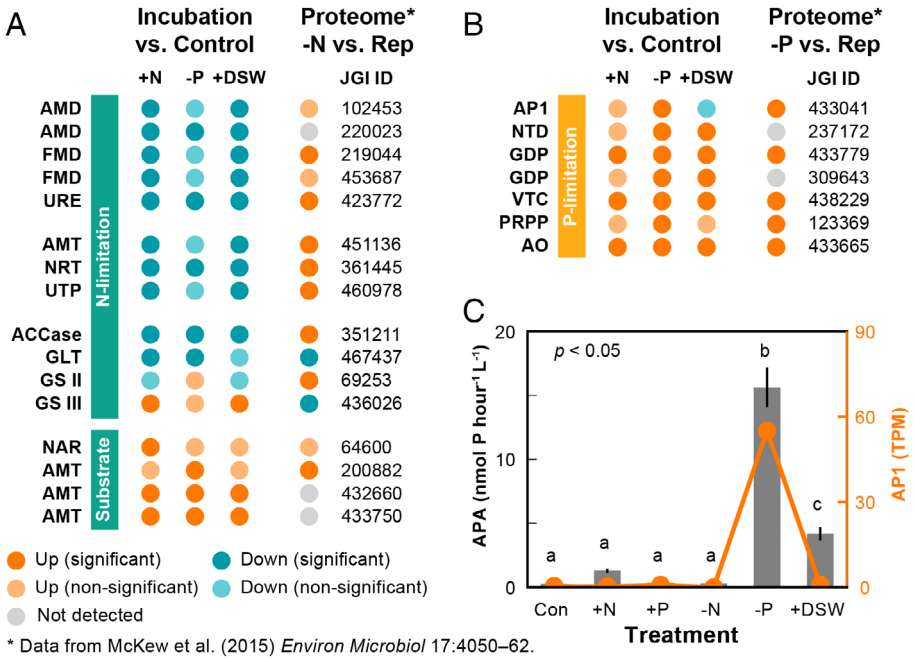

Fig. 3. Coordination between lab-based proteomic studies of nitrogen and phosphorus limitation in CCMP1516, bulk enzymatic activity, and patterns of transcript abundance in the field. The relative regulation and significance of OGs associated with nitrogen (N) limitation and substrate response (A) and with phosphorus (P) limitation (B) are shown for each of +N, −P, and deep seawater (+DSW) treatments compared to the unamended control. Additionally, the regulation of proteins from the proteomic study of McKew *et al*. (2015) is shown with comparisons of N-limited and P-limited cultures to nutrient replete cultures of CCMP1516. The bulk community alkaline phosphatase activity (APA) at the time of RNA sampling (7 days) was assessed for each of the six treatments in E2 (C). Significant differences in APA are marked with a, b, and c (Tukey HSD, $p < 0.05$). The relative transcript abundance in transcripts per million (TPM) for *E. huxleyi* AP1 is plotted in orange for each of the samples.

expressed in *E. huxleyi* both in N-limited cultures and in this oligotrophic setting, may be a unique and niche-defining aspect of *E. huxleyi*'s response to changes in N.

An exception to the coordination observed between the field data and other culture-based transcriptomic studies (Dyhrman *et al*., 2006; Rokitta *et al*., 2014) and proteomic studies (McKew *et al*., 2015) was a set of transporters [three groups of ammonium transporters (AMTs) and a nitrite/formamide transporter (NAR)] that had significantly increased abundance following N-addition (Fig. 3A). It may be that there are differences in transporter localization, and affinity with different *E. huxleyi* NAR and AMT lineages, and this could be the basis for the regulation difference observed here. When comparing field patterns to culture controls differences may also be attributed to other factors including differences in strain-composition in the field population and variation in the diel period at the time of sampling (Hernández Limón *et al*., 2020). One potential driver of the observed differences is that unlike culture studies done on axenic isolates, these microcosm experiments were performed with whole seawater, consisting of mixed communities of heterotrophic, mixotrophic, and autotrophic organisms. Over the course of the experiment, it is likely that there was active remineralization (Casciotti *et al*., 2008) that may have produced ammonium or amides that promoted the increase in these transporters.

The coordination of the N-induced transporters, enzymes used for the scavenging of N from organic molecules and shifts in energy metabolism strongly suggest that the *in situ* population of *E. huxleyi* was N-limited. These observations provide an unprecedented view of the importance of N in controlling the molecular physiology of *E. huxleyi* in the NPSG. Moreover, the choreography observed in the patterns of gene regulation between laboratory studies with axenic, monoclonal cultures and field microcosm experiments with mixed communities is striking and suggests that these responses are highly conserved within *E. huxleyi*.

Phosphorus scavenging

The dissolved N:P ratio was elevated relative to the control treatment in the +N, +DSW and −P treatments, the last of which represented the most extreme shift in N:P ratio (Supporting Information Fig. S1). OGs associated with P-metabolism and known to be P-regulated in culture-based studies (Dyhrman *et al*., 2006; McKew *et al*., 2015) showed a global trend towards increased abundance following N-addition, particularly in the −P treatment with the most extreme N:P ratio. Significant increases were observed in OGs associated with P-transport, P-scavenging from organic molecules, and polyphosphate (poly-P) metabolism (Fig. 2). A family of vacuolar transport chaperons (VTC) that contain the SPX domain, which are thought to be associated with poly-P metabolism (Ogawa *et al*., 2000; Hothorn *et al*., 2009; Dyhrman *et al*., 2012), had the largest significant increase in fold change in each of the treatments to which N was added (Fig. 2). Although poly-P accumulation is generally thought to be a luxury uptake response (Perry, 1976), VTC expression has been observed to be increased under P limitation in other studies (Dyhrman *et al*., 2006, 2012) and may be indicative of internal poly-P cycling. This is consistent with recent observation of enhanced bulk poly-P relative to total particulate P in low P regions like the NPSG and the Sargasso Sea (Martin *et al*., 2014; Diaz *et al*., 2016).

OGs associated with the scavenging of inorganic phosphate (P*i*) from organic molecules were also significantly increased, with two glycerophosphoryl diester phosphodiesterase (GDP) OGs and a 5′-nucleotidase (NTD) OG significantly more abundant following N-addition (Fig. 2). Additionally, two P-regulated gene families that are well-characterized in *E. huxleyi*, alkaline phosphatase (AP1) (Dyhrman and Palenik, 2003; Xu *et al*., 2006) and a phosphate-repressible phosphate permease (PRPP) (Chung *et al*., 2003; Dyhrman *et al*., 2006), were significantly increased only in the -P treatment (Fig. 2). This suggests that high-affinity P transport and the hydrolysis of phosphomonoesters like nucleotides are central to the low P response in *E. huxleyi*. These responses appear to be highly conserved, as they have also been observed in diatoms and pelagophytes (Wurch *et al*., 2011; Dyhrman *et al*., 2012).

As with the genes associated with N limitation, genes associated with P limitation were well choreographed with the proteomic data from the study by McKew *et al*. (2015) (Fig. 3B). Each of the OGs that was identified as significantly increased in the −P treatment was also identified as significantly increased in the P-limited cultures of CCMP1516, with the exception of two gene families (NTD and GDP), which were likely below their detection limit or lost during the extraction because of membrane association (Fig. 3B). Notably, NTD, which was not detected by McKew *et al*. (2015) in CCMP1516, was found to be present in *E. huxleyi* CCMP374 and CCMP373, and induced under P limitation (Dyhrman and Palenik, 2003). Similarly, in *E. huxleyi* cultures, PRPP has been found to be induced under low P conditions at both the transcript- (Dyhrman *et al*., 2006) and protein-levels (McKew *et al*., 2015), as well as in cultures grown on organic nitrogen (Bruhn *et al*., 2010).

The regulation of *E. huxleyi* AP1 showed particular sensitivity to the presence of P*i* in the environment as it was only significantly increased in the −P treatment (Fig. 3B and C). Alkaline phosphatase is a cell surface protein used for scavenging organic P from the environment and its induction in low P conditions is seen in

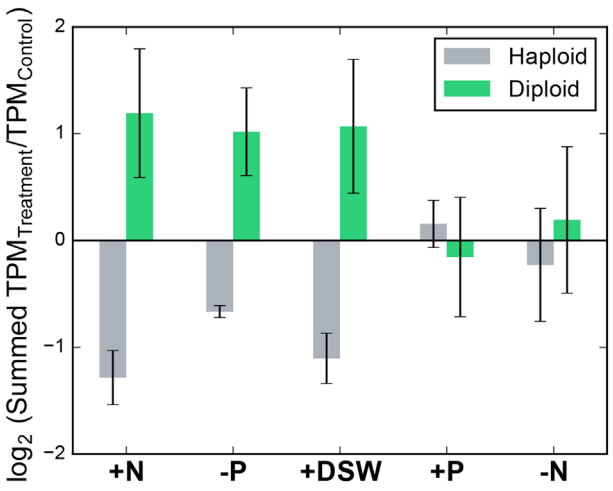

Fig. 4. Expression of haploid- and diploid-specific gene sets. OGs were identified as similar (e-value <1e-10) to the haploid-specific and diploid-specific EST clusters as defined by von Dassow *et al*. (2015), with 3491 and 4218 OGs identified, respectively (Supplementary Dataset S6). The transcripts per million (TPM) of all of the OGs for each of the groups was summed for each of the haploid- and diploid-specific gene sets in each of the microcosm treatments. Each nutrient-amended treatment was compared to the unamended control. The $\log_2$ of the mean fold change is reported for each treatment type, where standard deviation bars indicate the variability between the two replicated experiments (E1 and E2).

many diverse phytoplankton groups (Sakshaug *et al*., 1984; Dyhrman and Palenik, 1997, 2003; Wurch *et al*., 2011). AP1 in *E. huxleyi* has been shown to be increased 1000-fold at the transcript-level in low P conditions (Xu *et al*., 2006) and was found to constitute 3% of all spectral counts in a P-limited proteomic dataset (McKew *et al*., 2015). In +DSW, there was a slight decrease in AP1 transcript abundance (Fig. 3B), consistent with there being higher P*i* in the +DSW treatment than in the unamended control, −P, and + N treatments (Supporting Information Fig. S1). Additionally, bulk community alkaline phosphatase activity (APA) was significantly increased in the -P treatment relative to all other treatments (Tukey HSD, $P < 0.05$) and tracked well with the AP1 transcript abundance (Fig. 3C). The difference between bulk community activity and transcript abundance in the +DSW treatment underscores the power of species-specific methods, suggesting that other organisms in the community might be less sensitive to the presence of P*i*. This falls in line with previous findings that suggest that *E. huxleyi* may have one of the highest affinities (amongst eukaryotic algae) for P*i*, leading to its success in P-limited competition experiments (Riegman *et al*., 2000) and potentially enabling its ability to bloom in low P environments (Lessard *et al*., 2005). *Emiliania huxleyi* appears to be primarily limited by N, with P being a secondarily limiting factor in this region (Fig. 6).

Life-cycle and calcification

In recent years, the haplo-diplonic life cycle of *E. huxleyi*, wherein a cell switches between calcified diploid (2N) cells and non-calcified, flagellated haploid (1N) cells (Green *et al*., 1996), has been found to directly impact the photosynthetic response (Houdan *et al*., 2005), nutrient physiology (Rokitta *et al*., 2014, 2016), and global transcriptional signatures (von Dassow *et al*., 2009) of *E. huxleyi*. *In situ* surveys of the life-cycle dynamics of coccolithophores have suggested both biotic (viral-pressure) (Frada *et al*., 2012) and seasonal (Šupraha *et al*., 2016) controls on the life-cycle of the populations. Further, recent work has demonstrated the evolutionary erosion of haploid-specific genes from many oligotrophic lineages of *E. huxleyi*, leading to the inability to form flagellated cells in low nutrient ocean regimes (von Dassow *et al*., 2015). We leveraged the haploid- and diploid-specific gene sets described in the study by von Dassow *et al*. (2009, 2015) to identify sets of 3491 and 4218 haploid- and diploid-specific OGs in our reference data set (Supplementary Dataset S6). The summed expression (TPM) of both the total set of haploid- and the total set of diploid-specific OGs was tracked across each of the nutrient amended treatments relative to the expression observed in the unamended control. The haploid- and diploid-specific OG sets were found to co-occur across both of the experiments (E1 and E2). This finding is consistent with previous work that demonstrated the co-occurrence of haploid (heterococcolith) and diploid (holococcolith) cells in field populations of coccolithophores (Daniels *et al*., 2014), although niche separation might occur (such as along depth gradients) (Cros and Estrada, 2013). Here, the relative transcript abundance of the diploid-specific OG set increased and the haploid-specific OG set decreased in each of the N-amended treatments (+N, −P, and +DSW) relative to the unamended control (Fig. 4). This finding suggests that changes in N availability may be related to life-cycle shifts *in situ*. The link between ploidy or life phase and nutrient concentration is not well understood (Green *et al*., 1996), although a connection to viral infection has been hypothesized (Frada *et al*., 2008).

Concomitant with the observations of global ploidy state in the *E. huxleyi* population, shifts in genes associated with calcification were also observed (Fig. 5). Genes thought to be associated with calcification (Mackinder *et al*., 2010) and found to be up-regulated in calcifying cells (MacKinder *et al*., 2011) were found to be significantly increased following N-addition in the +N, −P, and + DSW treatments (Fig. 5). Although the addition of DSW was likely to have also shifted the carbonate chemistry of the system, there was little difference in the expression of known calcification genes between the nutrient amended treatments (+N and −P) and +DSW (Fig. 5 and Supplementary Dataset S5). These

genes included those associated with inorganic carbon transport [e.g. carbonic anhydrases (α-,β-, γ-, δ-CA) and a group of anion (Cl^-/HCO_3^-) exchangers (AE)], calcium (Ca) acquisition [e.g. voltage-gated Ca^{2+} channel (CAV), Na^+/Ca^{2+}-K^+ exchanger (NCKX), and Ca^{2+}/Mg^{2+}-permeable cation channel (CX)], proton transport [e.g. Vacuolar H^+-ATPase V_0 sector subunits c/c (ATPase)], and a putative calcium binding protein (GPA) (Fig. 5). These results are consistent with a potential shift in calcification. Such a pattern of increased calcification following N-addition is consistent with previously described coordination between nutrient environment and calcification in *E. huxleyi* (Paasche, 2002). For example, P-limitation has been observed to increase Ca content per coccolith and induce calcification in non-calcifying cultures (Müller *et al*., 2008; Rouco *et al*., 2013), while N limitation has been found to decrease Ca content per coccolith (Paasche and Brubak, 1994; Paasche, 1998).

In addition, the transcriptional markers suggest that N is a controlling factor in the life-cycle and calcification of *E. huxleyi* in the oligotrophic NPSG (Fig. 6). Von Dassow *et al*. (2015) noted that while the haploid phase is eroded in oligotrophic systems, it was not absent from all strains isolated in oligotrophic regions. Our results support this finding, suggesting that the haploid life stage persists within this oligotrophic NPSG population to some extent. Potentially, the

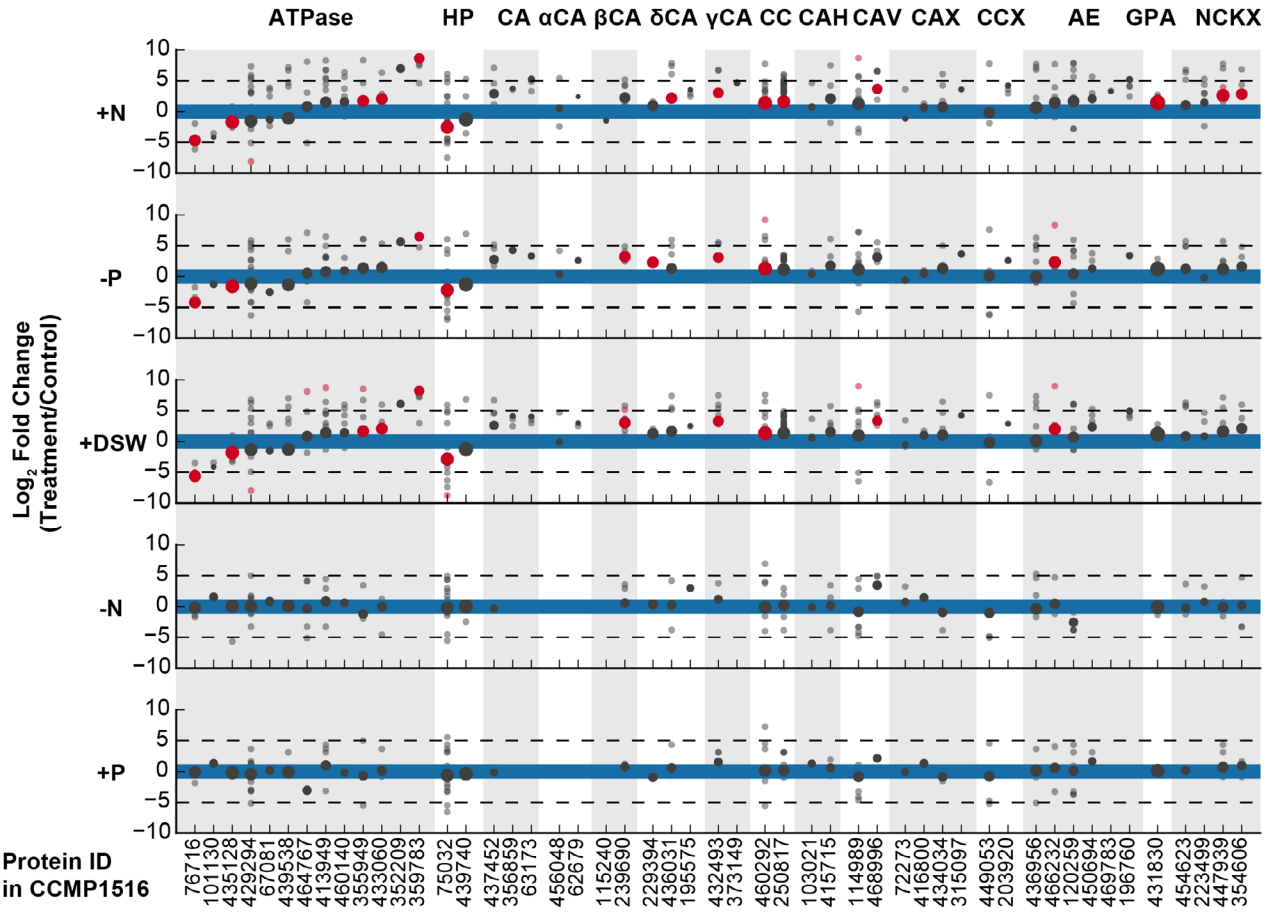

Fig. 5. Fold change of OGs associated with calcification in each of the amended microcosm treatments compared to the unamended control. The significance of log fold change of OGs associated with calcification (Supplementary Dataset S5), highlighted in blue, was assessed with edgeR across the five amended treatments relative to the unamended control. The size of the OG marker is proportional to the log of the mean abundance between the treatment and unamended control. OGs identified as significantly differently abundant between the treatment and the control, with a false discovery rate (FDR) < 0.05, are highlighted in red, whereas all others are plotted in dark grey. Individual transcripts within each OG are plotted in line vertically with the marker for the OG in either light grey or light red. As with the OGs, individual transcripts are highlighted in red if they are significantly differentially abundant between samples (FDR < 0.05). The x-axis labels indicate a representative protein id from the genome strain CCMP1516 for each of the OGs. OGs are grouped based on their general functions, which are listed as abbreviations across the top of the plot and alternately shaded in grey to aid visualization. The abbreviations are as follows: Plasma membrane H^+ATPase and/or vacuolar H^+ATPases (ATPase), H^+-translocating pyrophosphatase (HP), Carbonic anhydrase, not categorized (CA), α-type carbonic anhydrase (αCA), β-type carbonic anhydrase (βCA), δ-type carbonic anhydrase (δCA), γ-type carbonic anhydrase (γCA), Ca^{2+}/Mg^{2+}-permeable cation channels (CC), Ca^{2+}/H^+ antiporter (CAH), voltage-gated Ca^{2+} channel (CAV), Cation/Ca^{2+} exchanger (CCX), Anion (Na^+-independent Cl^-/HCO_3^-) exchanger (AE), Glutamic acid, proline, and alanine rich Ca^{2+} binding protein (GPA), Na^+/Ca^{2+}-K^+ exchanger (NCKX).

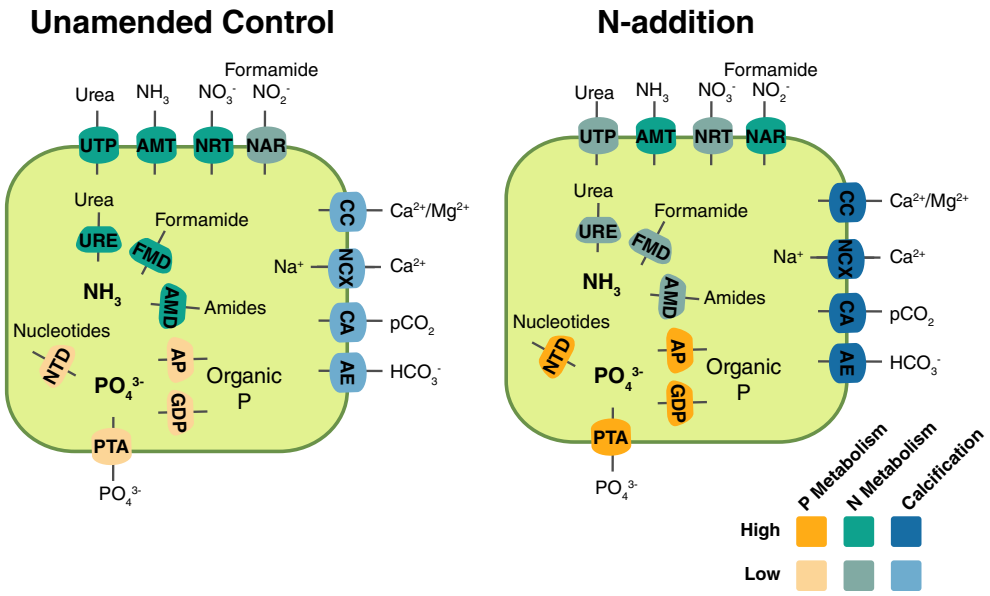

Fig. 6. Schematic cell model depicting the potential role of the transcripts described in this study in representative unamended control and N-addition treatments. The colour of the protein indicates which metabolic pathway is being represented: N-metabolism (green), P-metabolism (orange), and calcification (blue). The shade of the colour indicates whether a transcript was relatively high or low abundance in the treatment. The protein abbreviations are the same as used in Figs 2 and 5. Localization of proteins in the cell schematic does not necessarily represent protein localization in the cell.

haploid life stage persists in the oligotrophic environment due to differential nutrient niche partitioning between the diploid and haploid life stages, as described by Rokitta *et al*. (2014, 2016). Further work, coupling microscopic imaging, the measurement of calcification rates, and metatranscriptomic surveys, will serve to better characterize the exact nature of this transition.

Conclusions

Environmental perturbations in the NPSG (e.g. eddy-driven upwelling events) are known to induce shifts in the community composition and productivity (Brown *et al*., 2008). Here, we show that natural populations of *E. huxleyi* undergo transcriptional shifts in response to nutrient perturbations. These transcriptional shifts likely underlie plastic physiological responses used to adapt to new environmental conditions. The transcriptional patterns suggested that *E. huxleyi* populations in the NPSG were under N-control across the sampling period; primarily limited by N, with P being a secondarily limiting nutrient. The addition of N to these apparently N-limited communities evoked a strong transcriptional response that was well choreographed across experiments (Fig. 6) and mirrored previously observed patterns of metabolic remodelling from culture studies on individual isolates (Dyhrman and Palenik, 2003; Dyhrman *et al*., 2006; MacKinder *et al*., 2011; Rokitta *et al*., 2014; McKew *et al*., 2015). The transcriptional markers suggest that N is also a controlling factor on the life-cycle and calcification of *E. huxleyi* in the oligotrophic NPSG. N-flux in the future ocean may be critical in shaping *E. huxleyi* populations, particularly in subtropical gyres. Taken together, this study highlights the importance of transcriptional remodelling and phenotypic plasticity in the success of this coccolithophore.

Materials and methods

Sample collection and shipboard microcosm experiments

Seawater was collected at Station ALOHA (22°45′ N, 158°00′ W) from a depth of 25 m at 1400 h (local time) on two occasions during the summer of 2012, E1: 6 August and E2: 24 August, using a Eulerian sampling scheme as part of the Hawaii Ocean Experiment–Dynamics of Light and Nutrients (HOE-DYLAN) research expedition as per Alexander *et al*. (2015). These two dates represented the start of two factorial nutrient amendment microcosm experiments that were performed with natural communities to examine responses to shifting the ratios of the macronutrients, N and P. Triplicate, 20-L polycarbonate, clear carboys were amended with nutrients to generate the following conditions: +N: nitrate added (as $NaNO_3$); +P: phosphate added (as NaH_2PO_4 $2H_2O$); –N: phosphate, Fe, Si, and vitamin B_{12} added; -P: nitrate, Fe, Si, and vitamin B_{12} added; and +DSW: 10% v/v deep seawater added as described in Alexander *et al*. (2015); and Control: nothing added (Supporting Information Table S1).

Macronutrient additions were modelled after a simulated 10% deep seawater (DSW) upwelling as described in the study by Alexander *et al*. (2015). The concentration of iron was based on Marchetti *et al*. (2012) and vitamin B_{12} was modelled after Bertrand *et al*. (2007). Triplicate 20-L carboys of each condition were incubated at 30% surface light-levels using on-deck incubators for 7 days and processed on the final day for metatranscriptomics and ancillary measurements at 1400 h (local time) as per Alexander *et al*. (2015). Samples for dissolved nutrient concentrations for phosphate [PO_4^{3-}], nitrate and nitrite [$NO_2^- + NO_3^-$] were collected by filtering 125 ml of seawater through a 0.2 μm, 47 mm polycarbonate filter (Whatman), and stored frozen (–20°C) in acid-washed bottles until analysis. Nutrient samples were analysed by the Nutrient Analytical Services Laboratory at the Chesapeake Bay Lab (University of Maryland) following methods of the US EPA. Likewise, samples for alkaline phosphatase activity (APA) were collected by filtering 250 ml of whole seawater onto 0.2 μm, 47 mm polycarbonate filters and stored (–20°C) prior to analysis. These filters were then resuspended in artificial seawater and assayed for APA fluorometrically using the fluorogenic phosphatase substrate 6,8-difluoro-4-methylumbelliferyl phosphate (diMUF-P, ThermoFisher) following established field protocols (Dyhrman and Ruttenberg, 2006). Chlorophyll *a* was measured on whole water samples collected from water prior to the start of the incubation (T_0), the control, and the nutrient amendment treatments and filtered onto 25 mm GF/F filters (Whatman) using a 90% acetone extraction and assayed by fluorescence using an AquaFluor hand-held fluorometer (Turner Designs) (Parsons *et al*., 1984). The fluorometer was calibrated using chlorophyll *a* from *Anacystis nidulans* algae (Sigma).

RNA extraction and sequencing

RNA was extracted from individual filters with the RNeasy Mini Kit (Qiagen), following the protocol described in the study by Alexander *et al*. (2015). Extracted RNA was then pooled across triplicate carboys, representing approximately 56 L of seawater filtered per condition. Total RNA was enriched for eukaryotic mRNA through a poly-A pull down step and libraries were prepared with the Illumina TruSeq Library Prep Kit (Illumina). Libraries were sequenced with the Illumina HiSeq2000 at the JP Sulzberger Genome Center (CUGC) of Columbia University following Center protocols. Each sample was sequenced to produce 60 million, 100 base pair, paired-end reads (Supporting Information Table S2). All raw sequence data are available on the SRA under BioProject number PRJNA278441. Raw sequence data quality was visualized using FastQC and then cleaned and trimmed using Trimmomatic v 0.27 (paired end mode; 6-base pair wide sliding window for quality below 20; minimum length 25 base pair).

Reference data set preparation

The reference transcriptomes from unialgal cultures of four strains of *E. huxleyi*, CCMP374, CCMP379, CCMP370, and PLYM219 (Supporting Information Table S3), were collected from the MMETSP. The combined assemblies, as assembled with the National Center for Genome Resources (NCGR) pipeline on 4 September 2013, along with predicted protein translation and annotations are available through the iMicrobe data commons (Supporting Information Table S3). These reference transcriptomes were additionally annotated against the NCBI KOG database (2/2011) using rpsblast (v. 2.2.15, –e 0.001). In addition to these four reference transcriptomes, the predicted transcripts and proteins from the *E. huxleyi* genome strain CCMP1516 were used. The set of predicted protein translations for each of the reference transcriptomes was used for quality control and gene clustering. Each of the translated reference transcriptomes was trimmed based on predicted peptide length, requiring sequences to be longer than 70 amino acids. The resulting set of predicted proteins (and associated transcripts) was considered for subsequent analyses. Peptide sequences were clustered into gene clusters with orthoMCL (Li *et al*., 2003). OrthoMCL was run using BLASTP with an e-value cutoff of 1e-5 and an inflation value (-I) of 1.5 that was found to be optimized for the identification of OG.

Read mapping and analysis

Using the orthoMCL clustering framework, the relative expression of genes from *E. huxleyi* was tracked at two levels: (i) the OG, which considers the summed signature of all transcripts across strains based on orthology, and (ii) the transcript, which is specific to a single transcript within an OG. With this clustering framework, reads from the two replicated experiments were mapped to the curated *E. huxleyi* reference data set using RNA-Seq by Expectation Maximization (RSEM), a software package designed to estimate gene (here defined as OG) and isoform (here defined as strain-specific transcript) expression values from RNA-Seq data (Li and Dewey, 2011). Reads were mapped using bowtie2 version 2.1.10 called through the RSEM version 1.2.20 using the command rsem-calculate-expression with the parameters: –paired-end -p8 -bowtie2 -bowtie2-mismatch-rate 0.1. For each of the samples, this generated both alignment files (bam files) and files containing the gene and isoform level expression estimates. RSEM provides estimates of both the total number of fragments (reads) for a given isoform or gene, as well as of the

transcript fraction as a function of the size of the library, given in transcripts per million (TPM). The estimated TPM abundances were thus normalized across all samples and used for assessing relative abundance of the haploid-diploid gene sets (e.g. Figure 4).

Differentially abundant OGs and transcripts between replicated, experimental treatments were detected using edgeR. The programme edgeR is designed for the detection of differential expression between experiments with replicated sequencing data sets (Robinson *et al*., 2009) and applies a trimmed mean of M-values (TMM) normalization strategy that minimizes the fold change between samples for most genes, under the assumption that the majority of genes are not differentially regulated between samples (Robinson and Oshlack, 2010). Thus, edgeR takes into account both the original library size and a scaling factor to account for biological variability. Taking a conservative approach, data from like treatments from the two replicated experiments, E1 and E2, which were conducted with different communities from separate water masses more than 2 weeks apart, were considered to be biological replicates for differential abundance analysis. In this analysis, edgeR (Robinson *et al*., 2009) was applied with default parameters to calculate dispersion and to assess differential abundance of both specific transcripts and OGs of each of the treatments compared to the unammended control.

Genes previously associated with nitrogen and phosphorus metabolism (Dyhrman *et al*., 2006; Rokitta *et al*., 2014; McKew *et al*., 2015) and with calcification (MacKinder *et al*., 2011) in these previous studies were compared against the translated protein dataset comprising the OGs used in this study (tblastn with an e-value cutoff of 1e-20) to identify OGs associated with the aforementioned metabolic functions. Additionally, to investigate potential shifts in ploidy in the field, the predicted protein dataset used in this study was blasted (tblastn, e-value <1e-10) against 4552 and 4589 haploid- and diploid-specific EST clusters identified in strain RCC1216/1217 by von Dassow *et al*. (2009, 2015). OGs that were identified as common to both the haploid- and diploid- EST clusters were excluded. This yielded 3491 and 4218 haploid- and diploid-specific OGs, respectively.

Acknowledgements

H.A. was supported by the Department of Defence (DoD) through the National Defence Science & Engineering Graduate Fellowship (NDSEG) Program. This research was supported by funds from the Center for Microbial Oceanography Research and Education (CMORE, NSF EF04-24599) and from the Simons Foundation (SCOPE award ID 329108 to STD) and is a contribution of SCOPE. Support was also provided by the Gordon and Betty Moore Foundation through Grant #2637 to the National Center for Genome Resources for Marine Microbial Eukaryote Sequencing Program (MMETSP). The MMETSP samples used in this study were sequenced, assembled and annotated with the ABySS pipeline at the National Center for Genome Resources. The authors thank the captain and crew of the R/V Kilo Moana and the participants in the HOE-DYLAN cruise series for their help. The authors also thank Bethany Jenkins and Elizabeth Kujawinski for useful discussion.

Author contributions

Sample scheme and experiments were designed by S.T.D. and H.A. S.T.D., H.A., M.R.M., and S.T.H. collected samples and performed experiments. H.A. processed samples, created the databases, developed the bioinformatics pipeline, and performed data analysis. H.A. and S.T.D. wrote the paper with input from all co-authors.

References

Alexander, H., Rouco, M., Haley, S.T., Wilson, S.T., Karl, D. M., and Dyhrman, S.T. (2015) Functional group-specific traits drive phytoplankton dynamics in the oligotrophic ocean. *Proc Natl Acad Sci* **112**: E5972–E5979.

Behrenfeld, M.J., O'Malley, R.T., Siegel, D., McClain, C.R., Sarmiento, J.L., Feldman, G.C., *et al*. (2006) Climate-driven trends in contemporary ocean productivity. *Nature* **444**: 752–755.

Bertrand, E.M., Saito, M.A., Rose, J.M., Riesselman, C.R., Lohan, M.C., Noble, A.E., *et al*. (2007) Vitamin B12 and iron colimitation of phytoplankton growth in the Ross Sea. *Limnol Oceanogr* **52**: 1079–1093.

Bollmann, J., and Herrle, J.O. (2007) Morphological variation of *Emiliania huxleyi* and sea surface salinity. *Earth Planet Sci Lett* **255**: 273–288.

Brown, C.W., and Yoder, J.A. (1994) Coccolithophorid blooms in the global ocean. *J Geophys Res* **99**: 7467–7482.

Brown, S.L., Landry, M.R., Selph, K.E., Jin Yang, E., Rii, Y. M., and Bidigare, R.R. (2008) Diatoms in the desert: plankton community response to a mesoscale eddy in the subtropical North Pacific. *Deep Res Part II Top Stud Oceanogr* **55**: 1321–1333.

Bruhn, A., LaRoche, J., and Richardson, K. (2010) *Emiliania huxleyi* (Prymnesiophyceae): nitrogen-metabolism genes and their expression in response to external nitrogen sources. *J Phycol* **46**: 266–277.

Casciotti, K.L., Trull, T.W., Glover, D.M., and Davies, D. (2008) Constraints on nitrogen cycling at the subtropical North Pacific Station ALOHA from isotopic measurements of nitrate and particulate nitrogen. *Deep Res Part II Top Stud Oceanogr* **55**: 1661–1672.

Chung, C.C., Hwang, S.P.L., and Chang, J. (2003) Identification of a high-affinity phosphate transporter gene in a prasinophyte alga, *Tetraselmis chui*, and its expression under nutrient limitation. *Appl Environ Microbiol* **69**: 754–759.

Cortés, M.Y., Bollmann, J., and Thierstein, H.R. (2001) Coccolithophore ecology at the HOT station ALOHA Hawaii. *Deep Res Part II Top Stud Oceanogr* **48**: 1957–1981.

Cros, L., and Estrada, M. (2013) Holo-heterococcolithophore life cycles: ecological implications. *Mar Ecol Prog Ser* **492**: 57–68.

Daniels, C.J., Tyrrell, T., Poulton, A.J., and Young, J.R. (2014) A mixed life-cycle stage bloom of *Syracosphaera bannockii* (Borsetti and Cati, 1976) Cros et al . 2000 (Bay of Biscay, April 2010). *J Nannoplankt Res* **34**: 31–35.

von Dassow, P., John, U., Ogata, H., Probert, I., Bendif, E. M., Kegel, J.U., *et al*. (2015) Life-cycle modification in open oceans accounts for genome variability in a cosmopolitan phytoplankton. *ISME J* **9**: 1365–1377.

von Dassow, P., Ogata, H., Probert, I., Wincker, P., Da Silva, C., Audic, S., *et al*. (2009) Transcriptome analysis of functional differentiation between haploid and diploid cells of *Emiliania huxleyi*, a globally significant photosynthetic calcifying cell. *Genome Biol* **10**: R114.

Diaz, J.M., Björkman, K.M., Haley, S.T., Ingall, E.D., Karl, D. M., Longo, A.F., and Dyhrman, S.T. (2016) Polyphosphate dynamics at station ALOHA, North Pacific subtropical gyre. *Limnol Oceanogr* **61**: 227–239.

Duce, R.A., LaRoche, J., Altieri, K., Arrigo, K.R., Baker, A. R., Capone, D.G., *et al*. (2008) Impacts of atmospheric anthropogenic nitrogen on the Open Ocean. *Science (80-.).* **320**: 893–897.

Dyhrman, S.T., and Anderson, D.M. (2003) Urease activity in cultures and field populations of the toxic dinoflagellate *Alexandrium*. *Limnol Ocean* **48**: 647–655.

Dyhrman, S.T., Haley, S.T., Birkeland, S.R., Wurch, L.L., Cipriano, M.J., and McArthur, A.G. (2006) Long serial analysis of gene expression for gene discovery and transcriptome profiling in the widespread marine coccolithophore *Emiliania huxleyi*. *Appl Environ Microbiol* **72**: 252–260.

Dyhrman, S.T., Jenkins, B.D., Rynearson, T.A., Saito, M.A., Mercier, M.L., Alexander, H., *et al*. (2012) The transcriptome and proteome of the diatom *Thalassiosira pseudonana* reveal a diverse phosphorus stress response. *PLoS One* **7**: e33768.

Dyhrman, S.T., and Palenik, B. (2003) Characterization of ectoenzyme activity and phosphate-regulated proteins in the coccolithophorid *Emiliania huxleyi*. *J Plankton Res* **25**: 1215–1225.

Dyhrman, S.T., and Palenik, B.P. (1997) The identification and purification of a cell-surface alkaline phosphatase from the dinoflagellate *Prorocentrum minimum* (Dinophyceae). *J Phycol* **33**: 602–612.

Dyhrman, S.T., and Ruttenberg, K.C. (2006) Presence and regulation of alkaline phosphatase activity in eukaryotic phytoplankton from the coastal ocean: implications for dissolved organic phosphorus remineralization. *Limnol Oceanogr* **51**: 1381–1390.

Feng, Y., Warner, M.E., Zhang, Y., Sun, J., Fu, F.X., Rose, J. M., and Hutchins, D.A. (2008) Interactive effects of increased pCO2, temperature and irradiance on the marine coccolithophore *Emiliania huxleyi* (Prymnesiophyceae). *Eur J Phycol* **43**: 87–98.

Field, C.B. (1998) Primary production of the biosphere: integrating terrestrial and oceanic components. *Science (80-.)* **281**: 237–240.

Frada, M., Probert, I., Allen, M.J., Wilson, W.H., and de Vargas, C. (2008) The "Cheshire cat" escape strategy of the coccolithophore *Emiliania huxleyi* in response to viral infection. *Proc Natl Acad Sci U S A* **105**: 15944–15949.

Frada, M.J., Bidle, K.D., Probert, I., and de Vargas, C. (2012) *In situ* survey of life cycle phases of the coccolithophore *Emiliania huxleyi* (Haptophyta). *Environ Microbiol* **14**: 1558–1569.

Frischkorn, K.R., Harke, M.J., Gobler, C.J., and Dyhrman, S. T. (2014) De novo assembly of *Aureococcus anophagefferens* transcriptomes reveals diverse responses to the low nutrient and low light conditions present during blooms. *Front Microbiol* **5**: 375.

Green, J.C., Course, P.A., and Tarran, G.A. (1996) The life-cycle of *Emiliania huxleyi*: a brief review and a study of relative ploidy levels analysed by flow cytometry. *J Mar Syst* **9**: 33–44.

Hernández Limón, M.D., Hennon, G.M.M., Harke, M.J., Frischkorn, K.R., Haley, S.T., and Dyhrman, S.T. (2020) Transcriptional patterns of *Emiliania huxleyi* in the North Pacific subtropical gyre reveal the daily rhythms of its metabolic potential. *Environ Microbiol* **22**: 381–396.

Holligan, P.M., Fernández, E., Aiken, J., Balch, W.M., Boyd, P., Burkill, P.H., *et al*. (1993) A biogeochemical study of the coccolithophore, *Emiliania huxleyi*, in the North Atlantic. *Global Biogeochem Cycles* **7**: 879–900.

Hothorn, M., Neumann, H., Lenherr, E.D., Wehner, M., Rybin, V., Hassa, P.O., *et al*. (2009) Catalytic core of a membrane-associated eukaryotic polyphosphate polymerase. *Science (80-.).* **324**: 513–516.

Houdan, A., Probert, I., Van Lenning, K., and Lefebvre, S. (2005) Comparison of photosynthetic responses in diploid and haploid life-cycle phases of *Emiliania huxleyi* (Prymnesiophyceae). *Mar Ecol Prog Ser* **292**: 139–146.

Keeling, P.J., Burki, F., Wilcox, H.M., Allam, B., Allen, E.E., Amaral-Zettler, L.A., *et al*. (2014) The Marine Microbial Eukaryote Transcriptome Sequencing Project (MMETSP): illuminating the functional diversity of eukaryotic life in the oceans through transcriptome sequencing. *PLoS Biol* **12**: e1001889.

Landry, D.M., Kristiansen, S., and Palenik, B.P. (2009) Molecular characterization and antibody detection of a nitrogen-regulated cell-surface protein of the coccolithophore *Emiliania huxleyi* (Prymnesiophyceae). *J Phycol* **45**: 650–659.

Lessard, E.J., Merico, A., and Tyrrell, T. (2005) Nitrate: phosphate ratios and *Emiliania huxleyi* blooms. *Limnol Oceanogr* **50**: 1020–1024.

Li, B., and Dewey, C.N. (2011) RSEM: accurate transcript quantification from RNA-Seq data with or without a reference genome. *BMC Bioinformatics* **12**: 323.

Li, L., Stoeckert, C.J., and Roos, D.S. (2003) OrthoMCL: identification of ortholog groups for eukaryotic genomes. *Genome Res* **13**: 2178–2189.

MacKinder, L., Wheeler, G., Schroeder, D., von Dassow, P., Riebesell, U., and Brownlee, C. (2011) Expression of biomineralization-related ion transport genes in *Emiliania huxleyi*. *Environ Microbiol* **13**: 3250–3265.

Mackinder, L., Wheeler, G., Schroeder, D., Riebesell, U., and Brownlee, C. (2010) Molecular mechanisms underlying calcification in coccolithophores. *Geomicrobiol J* **27**: 585–595.

Marchetti, A., Schruth, D.M., Durkin, C.A., Parker, M.S., Kodner, R.B., Berthiaume, C.T., *et al*. (2012) Comparative

metatranscriptomics identifies molecular bases for the physiological responses of phytoplankton to varying iron availability. *Proc Natl Acad Sci* **109**: E317–E325.

Martin, P., Dyhrman, S.T., Lomas, M.W., Poulton, N.J., and Van Mooy, B.A.S. (2014) Accumulation and enhanced cycling of polyphosphate by Sargasso Sea plankton in response to low phosphorus. *Proc Natl Acad Sci U S A* **111**: 8089–8094.

McKew, B.A., Metodieva, G., Raines, C.A., Metodiev, M.V., and Geider, R.J. (2015) Acclimation of *Emiliania huxleyi* (1516) to nutrient limitation involves precise modification of the proteome to scavenge alternative sources of N and P. *Environ Microbiol* **17**: 4050–4062.

Moore, C.M., Mills, M.M., Arrigo, K.R., Berman-Frank, I., Bopp, L., Boyd, P.W., *et al*. (2013) Processes and patterns of oceanic nutrient limitation. *Nat Geosci* **6**: 701–710.

Van Mooy, B., Fredricks, H.F., Pedler, B.E., Dyhrman, S.T., Karl, D.M., Koblízek, M., *et al*. (2009) Phytoplankton in the ocean use non-phosphorus lipids in response to phosphorus scarcity. *Nature* **458**: 69–72.

Müller, M.N., Antia, A.N., and LaRoche, J. (2008) Influence of cell cycle phase on calcification in the coccolithophore *Emiliania huxleyi*. *Limnol Oceanogr* **2008**: 506–512.

Ogawa, N., DeRisi, J., and Brown, P.O. (2000) New components of a system for phosphate accumulation and polyphosphate metabolism in *Saccharomyces cerevisiae* revealed by genomic expression analysis. *Mol Biol Cell* **11**: 4309–4321.

Paasche, E. (2002) A review of the coccolithophorid *Emiliania huxleyi* (Prymnesiophyceae), with particular reference to growth, coccolith formation, and calcification-photosynthesis interactions. *Phycologia* **40**: 503–529.

Paasche, E. (1998) Roles of nitrogen and phosphorus in coccolith formation in *Emiliania huxleyi* (Prymnesiophyceae). *Eur J Phycol* **33**: 33–42.

Paasche, E., and Brubak, S. (1994) Enhanced calcification in the coccolithophorid *Emiliania huxleyi* (Haptophyceae) under phosphorus limitation. *Phycologia* **33**: 324–330.

Palenik, B., and Henson, S.E. (1997) The use of amides and other organic nitrogen sources by the phytoplankton *Emiliania huxleyi*. *Limnol Oceanogr* **42**: 1544–1551.

Parsons, T.R., Maita, Y., and Lalli, C.M. (1984) *A Manual of Biological and Chemical Methods for Seawater Analysis*. Oxford: Pergamon Press.

Paytan, A., and McLaughlin, K. (2007) The oceanic phosphorus cycle. *Chem Rev* **107**: 563–576.

Perry, M.J. (1976) Phosphate utilization by an oceanic diatom in phosphorus-limited chemo-stat culture and in the oligotrophic waters of the central North Pacific. *Limnol Oceanogr* **21**: 88–107.

Polovina, J.J., Howell, E.A., and Abecassis, M. (2008) Ocean's least productive waters are expanding. *Geophys Res Lett* **35**: L03618.

Poulton, A.J., Adey, T.R., Balch, W.M., and Holligan, P.M. (2007) Relating coccolithophore calcification rates to phytoplankton community dynamics: regional differences and implications for carbon export. *Deep. Res. Part II Top. Stud. Oceanogr.* **54**: 538–557.

Read, B.A., Kegel, J., Klute, M.J., Kuo, A., Lefebvre, S.C., Maumus, F., *et al*. (2013) Pan genome of the phytoplankton *Emiliania* underpins its global distribution. *Nature* **499**: 209–213.

Riegman, R., Stolte, W., Noordeloos, A.A.M., and Slezak, D. (2000) Nutrient uptake, and alkaline phosphate (EC 3: 1: 3: 1) activity of *Emiliania huxleyi* (Prymnesiophyceae) during growth under N and P limitation in continuous cultures. *J Phycol* **36**: 87–96.

Robinson, M., and Oshlack, A. (2010) A scaling normalization method for differential expression analysis of RNA-seq data. *Genome Biol* **11**: 1–9.

Robinson, M.D., McCarthy, D.J., and Smyth, G.K. (2009) edgeR: a bioconductor package for differential expression analysis of digital gene expression data. *Bioinformatics* **26**: 139–140.

Rokitta, S.D., Von Dassow, P., Rost, B., and John, U. (2014) *Emiliania huxleyi* endures N-limitation with an efficient metabolic budgeting and effective ATP synthesis. *BMC Genomics* **15**: 1051.

Rokitta, S.D., Von Dassow, P., Rost, B., and John, U. (2016) P- and N-starvation trigger the same cellular responses to promote senescence in eukaryotic phytoplankton. *Front Mar Sci* **3**: 109.

Rouco, M., Branson, O., Lebrato, M., and Iglesias-Rodroguez, M.D. (2013) The effect of nitrate and phosphate availability on *Emiliania huxleyi* (NZEH) physiology under different CO_2 scenarios. *Front Microbiol* **4**: 155.

Ruttenberg, K.C. (2001) Phosphorus cycle. *Encycl Ocean Sci* **4**: 401–412.

Sakshaug, E., Granéli, E., and Kayser, M.E.H. (1984) Chemical composition and alkaline phosphatase activity of nutrient-saturated and P-deficient cells of four marine dinoflagellates. *J Exp Mar Bio Ecol* **77**: 241–254.

Sarmiento, J.L., Hughes, T.M.C., Stouffer, R.J., and Manabe, S. (1998) Simulated response of the ocean carbon cycle to anthropogenic climate warming. *Nature* **393**: 245–249.

Sarmiento, J.L., Slater, R., Barber, R., Bopp, L., Doney, S. C., Hirst, A.C., *et al*. (2004) Response of ocean ecosystems to climate warming. *Global Biogeochem Cycles* **18**: GB3003.

Shemi, A., Schatz, D., Fredricks, H.F., Van Mooy, B.A.S., Porat, Z., and Vardi, A. (2016) Phosphorus starvation induces membrane remodeling and recycling in *Emiliania huxleyi*. *New Phytol* **211**: 886–898.

Simó, R. (2001) Production of atmospheric sulfur by oceanic plankton: biogeochemical, ecological and evolutionary links. *Trends Ecol Evol* **16**: 287–294.

Smil, V. (2000) Phosphorus in the environment: natural flows and human interferences. *Annu Rev Energy Environ* **25**: 53–88.

Šupraha, L., Ljubešić, Z., Mihanović, H., and Henderiks, J. (2016) Coccolithophore life-cycle dynamics in a coastal Mediterranean ecosystem: seasonality and species-specific patterns. *J Plankton Res* **38**: 1178–1193.

Wilson, S.T., Barone, B., Ascani, F., Bidigare, R.R., Church, M.J., Del Valle, D.A., *et al*. (2015) Short-term variability in euphotic zone biogeochemistry and primary productivity at station ALOHA: a case study of summer 2012. *Global Biogeochem Cycles* **29**: 1145–1164.

Wurch, L.L., Bertrand, E.M., Saito, M.A., van Mooy, B.A.S., and Dyhrman, S.T. (2011) Proteome changes driven by phosphorus deficiency and recovery in the brown tide-forming alga *Aureococcus anophagefferens*. *PLoS One* **6**: e28949.

Xu, Y., Wahlund, T.M., Feng, L., Shaked, Y., and Morel, F. M.M. (2006) A novel alkaline phosphatase in the coccolithophore *Emiliania huxleyi* (Prymnesiophyceae) and its regulation by phosphorus. *J Phycol* **42**: 835–844.

Zondervan, I. (2007) The effects of light, macronutrients, trace metals and CO2 on the production of calcium carbonate and organic carbon in coccolithophores-a review. *Deep Res Part II Top Stud Oceanogr.* **54**: 521–537.

Zondervan, I., Zeebe, R.E., Rost, B., and Riebesell, U. (2001) Decreasing marine biogenic calcification: a negative feedback on rising atmospheric pCO2. *Global Biogeochem Cycles* **15**: 507–516.

Supporting Information

Additional Supporting Information may be found in the online version of this article at the publisher's web-site:

Supplementary Figure S1 Inorganic nitrogen and phosphorus concentrations at the point of RNA sampling (7 days post-inoculation) for each of the six microcosm treatments in E1 and E2, averaged across triplicate carboys. Average and standard deviation are reported (n = 3).

Supplementary Figure S2 Chlorophyll *a* at the point of RNA sampling (T_0 and 7 days post-inoculation) for each of the six treatments in E1 and E2, averaged across triplicate carboys. Average and standard deviation are reported (n = 3).

Supplementary Figure S3 (A-E) Statistical significance of the log average abundance and log fold change for each of the detected *E. huxleyi* transcripts was assessed between the unamended control relative to the amended treatments: (A) + N, (B) -P, (C) + DSW, (D) -N, and (E) + P. Transcripts that are identified as significantly increased or decreased, with a false discovery rate (FDR) < 0.05, in a treatment relative to the control are highlighted in orange while those not significantly changed are grey. (F) A weighted Venn diagram comparing the composition of the significantly (FDR < 0.05) differentially abundant transcripts across each of the amendments to which N was added (A-C) compared to the unamended control, with the size of the circles scaled to the relative number of differentially abundant transcripts within a treatment.

Supplementary Table S1. Nutrient concentrations added to the in nutrient-amended microcosm treatments.

Supplementary Table S2.. Sequence library information for each sample.

Supplementary Table S3. Strain isolation date, synonyms, and transcriptome/genome information for each of the five strains used in this study.

Supplementary Dataset S1. The membership of each orthologous group (OG) across the five strains surveyed in this study (CCMP379, PLYM219, CCMP370, CCMP374 and CCMP1516).

Supplementary Dataset S2. The RSEM estimated counts, RSEM estimated transcripts per million (TPM), and KEGG and KOG annotations for each of the orthologous groups (OGs) across each of the *in situ* samples and microcosm experiments.

Supplementary Dataset S3. The edgeR estimated $\log_2$ fold change, $\log_2$ counts-per-million, FDR, and *p*-value for each orthologous group (OG) in each of the amended microcosm experiments compared to the unamended control.

Supplementary Dataset S4. The edgeR estimated log2 fold change, log2 counts-per-million, FDR, and *p*-value for each transcript in each of amended microcosm treatments compared to the unamended control.

Supplementary Dataset S5. The edgeR estimated log2 fold change and FDR, isoform, and annotation data for genes associated with nitrogen, phosphorus, calcification, as plotted in Figs 2 and 5.

Supplementary Dataset S6. The haploid- and diploid-specific EST clusters identified by von Dassow *et al*. (2014), protein best-hit (tblastn, e-value < e-10), and associated orthologous groups